Abstracta

Ano IX - N. 03

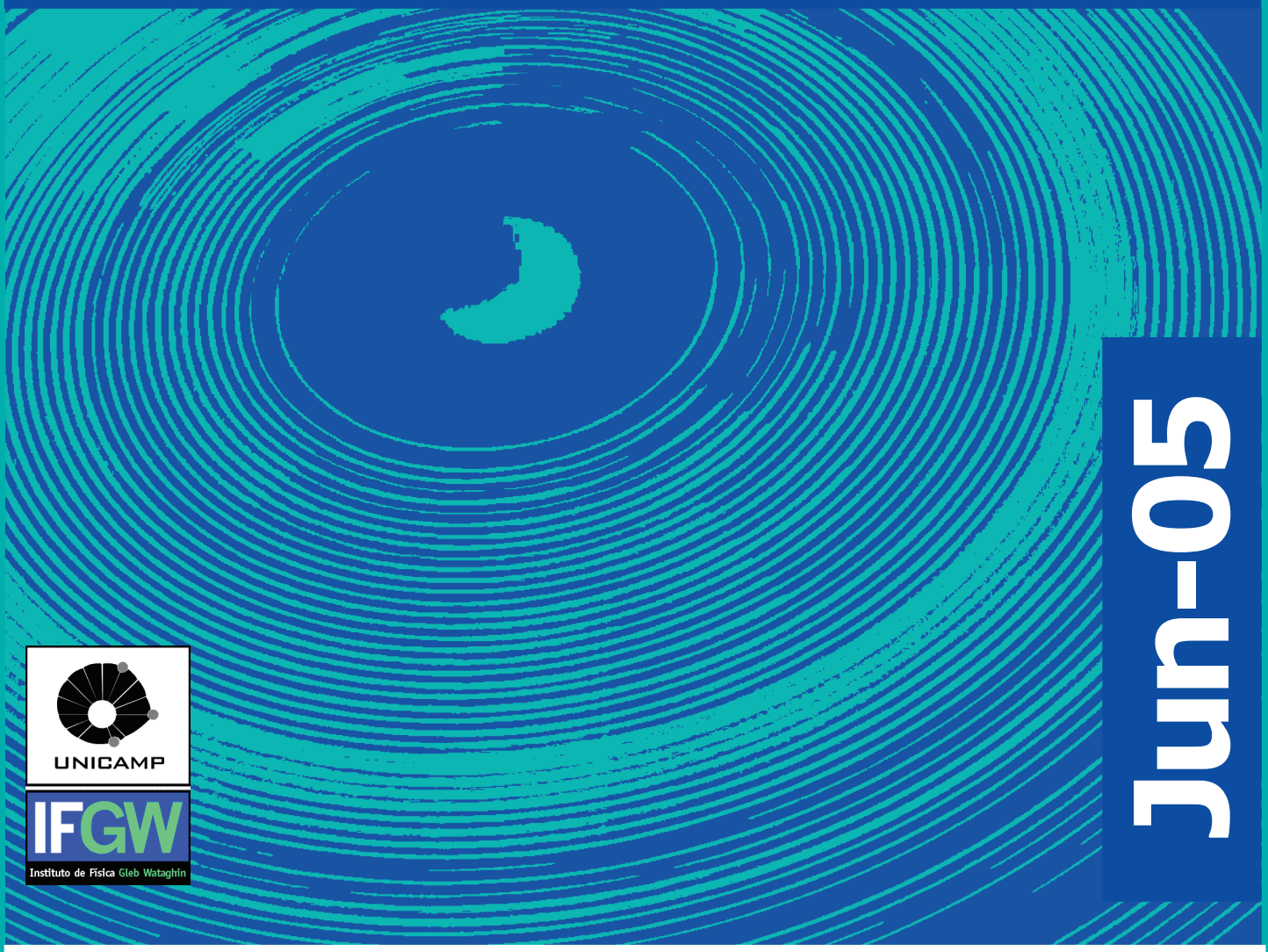

Jun-05

UNICAMP

IFGW
Instituto de Física Gleb Wataghin

TRABALHOS PUBLICADOS

Abril 2005 à Maio 2005
P 083 à P 131 / 2005

TRABALHOS ACEITOS PARA PUBLICAÇÃO

A 001- 05 Statistical approach to fractal-structured systems: an illustratrion from the physics of semiconductor heterostructures.
C 001- 05 Planar waveguides prepared with organic-inorganic sol-gel derived from carboxylic acid solvolysis.

TRABALHOS PUBLICADOS

P083-05 "Absence of conventional quantum phase transitions in itinerant systems with disorder"

Dobrosavljevic, V. and Miranda, E.

Effects of disorder are examined in itinerant systems close to quantum critical points. We argue that spin fluctuations due to the long-range part of the RKKY interactions generically induce non-Ohmic dissipation due to rare disorder configurations. This dissipative mechanism is found to destabilize quantum Griffiths phase behavior in itinerant systems with arbitrary symmetry of the order parameter, leading to the formation of a "cluster glass" phase preceding uniform ordering.

Physical Review Letters 94[18]. 187203. 2005.

P084-05 "Analytical model to understand the colossal magnetocaloric effect"

von Ranke, P. J., de Oliveira, N. A., Mello, C., Carvalho, A. M. G., and Gama, S.

We report the theoretical investigations on the colossal magnetocaloric effect using a simple model that couples the lattice entropy and magnetic entropy through the magnetoelastic deformation. Analytical expressions were obtained for the thermodynamic magnetic state equation as well as for the total entropy and heat capacity. The coupled magnetic lattice model predicts high isothermal entropy changes due to the lattice contribution for external magnetic field change, overcoming the magnetic entropy change limit.

Physical Review B 71[5]. 054410. 2005.

P085-05 "Band gap engineering for poly(p-phenylene) and poly(p-phenylene vinylene) copolymers using the tight-binding approach"

Giro, R., Caldas, M. J., and Galvao, D. S.

The interest in poly(p-phenylene) (PPP) and poly(p-phenylene vinylene) (PPV) copolymers stems from the fact that these homopolymers present interesting optical and electronic properties that allow a great variety of technological applications. Combining different numbers of PPP and PPV units it is possible, in principle, to obtain new structures presenting intermediate gap values (2.8 eV and 2.4 eV for PPP and PPV, respectively). For this study we used a Huckel Hamiltonian tight-binding coupled to the negative factor counting (NFC) technique. We carried out a systematic search to determine optimum relative concentrations for disordered binary polymeric alloys with predefined gap values. Once these structures were obtained, we used the semiempirical methods AM1/PM3 and ZINDO/S-CI for geometrical and optical studies, respectively. Our theoretical results show that it is possible to obtain copolymers of PPP and PPV with intermediate gap values of their parent structures.

International Journal of Quantum Chemistry 103[5], 588-596. 2005.

P086-05 "Carcinogenic classification of polycyclic aromatic hydrocarbons through theoretical descriptors"

Troche, K. S., Braga, S. F., Coluci, V. R., and Galvao, D. S.

Polycyclic aromatic hydrocarbons (PAHs) constitute an important family of molecules capable of inducing chemical carcinogenesis. In this work we report a comparative structure-activity relationship (SAR) study for 81 PAHs using different methodologies. The recently developed electronic indices methodology (EIM) with quantum descriptors obtained from different semiempirical methods (AM1, PM3, and PM5) was contrasted against more standard pattern recognition methods (PRMs), principal component analysis (PCA), hierarchical cluster analysis (HCA), Kth nearest neighbor (KNN), soft independent modeling of class analogies (SIMCA), and neural networks (NN). Our results show that PRMs validate the statistical value of electronic parameters derived from EIM analysis and their ability to identify active compounds. EIM outperformed more standard SAR methodologies and does not appear to be significantly Hamiltonian-dependent.

International Journal of Quantum Chemistry 103[5], 718-730. 2005.

P087-05 "Chaotic signature in the motion of coupled carbon nanotube oscillators"

Coluci, V. R., Legoas, S. B., de Aguiar, M. A. M., and Galvao, D. S.

The motion of coupled oscillators based on multiwalled carbon nanotubes is studied using rigid-body dynamics simulations. The results show the existence of chaotic and regular behaviours for a given total energy, indicating the manifestation of chaos in nanoscaled mechanical systems based on carbon nanotube oscillators. Different regular motions are observed for different total energies, and they can be obtained by appropriately choosing the initial conditions. This possibility can allow the construction of multi-functional nano-devices based on multiwalled carbon nanotube oscillators.

Nanotechnology 16[4], 583-589. 2005.

P088-05 "Characterization of new FIR laser lines from CHD2OH"

Viscovini, R. C., Cruz, F. C., and Pereira, D.

In this work, we report new optically pumped far-infrared (FIR) laser lines from CHD2OH. A waveguide CO2 laser of wide tunability (290 MHz) was used as pump source, and a Fabry-Perot open cavity was used as a FIR laser resonator. Optoacoustic absorption spectra were used as a guide to search for new FIR laser lines. We could observe 15 new laser lines in the range from 116.4 to 401.4 mu m. The lines were characterized according to wavelength, relative polarization, relative intensity, and optimum working pressure. The transferred Lamb-dip technique was used to measure the frequency absorption transition both for the new and previously reported laser lines.

IEEE Journal of Quantum Electronics 41[5], 694-696. 2005.

P089-05 "Diamond thermal expansion measurement using transmitted X-ray back-diffraction"

Giles, C., Adriano, C., Lubambo, A. F., Cusatis, C., Mazzaro, I., and Honnicke, M. G.

The linear thermal expansion coefficient of diamond has been measured using forward-diffracted profiles in X-ray backscattering. This experimental technique is presented as an alternative way of measuring thermal expansion coefficients of solids in the high-resolution Bragg backscattering geometry without the intrinsic difficulty of detecting the reflected beam. The temperature dependence of the lattice parameter is obtained from the high sensitivity of the transmitted profiles to the Bragg angle variation with temperature.

The large angular width of the backscattering profiles allows the application of this technique to mosaic crystals with high resolution. As an application of this technique the thermal expansion coefficient of a synthetic type-Ib diamond (110) single crystal was measured from 10 to 300 K. Extremely low values (of the order of 1 x 10(-7) +/- 5 x 10(-7)) for the linear thermal expansion coefficient in the temperature range from 30 to 90 K are in good agreement with other reported measurements.

Journal of Synchrotron Radiation 12[Pt-3], 349-353. 2005.

P090-05 "Dissipative dynamics of topological defects in frustrated Heisenberg spin systems"

Juricic, V., Benfatto, L., Caldeira, A. O., and Smith, C. M.

We study the dynamics of topological defects of a frustrated spin system displaying spiral order. As a starting point we consider the SO(3) nonlinear sigma model to describe long-wavelength fluctuations around the noncollinear spiral state. Besides the usual spin-wave magnetic excitations, the model allows for topologically nontrivial static solutions of the equations of motion, associated with the change of chirality (clockwise -or counterclockwise) of the spiral. We consider two types of these topological defects, single vortices and vortex-antivortex pairs, and quantize the corresponding solutions by generalizing the semiclassical approach to a non-Abelian field theory. The use of the collective coordinates allows us to represent the defect as a particle coupled to a bath of harmonic oscillators, which can be integrated out employing the Feynman-Vernon path-integral formalism, The resulting effective action for the defect indicates that its motion is damped due to the scattering by the magnons. We derive a general expression for the damping coefficient of the defect, and evaluate its temperature dependence in both cases, for a single vortex and for a vortex-antivortex pair. Finally, we consider an application of the model for cuprates, where a spiral state has been argued to be realized in the spin-glass regime. By assuming that the defect motion contributes to the dissipative dynamics of the charges, we can compare our results with the measured inverse mobility in a wide range of temperature. The relatively good agreement between our calculations and the experiments confirms the possible relevance of an incommensurate spiral order for lightly doped cuprates.

Physical Review B 71[6]. 064421. 2005.

P091-05 "Effects of non-standard neutrino interactions on MSW-LMA solution to the solar neutrino problem"

Guzzo, M. M., de Holanda, P. C., and Peres, O. L. G.

Nuclear Physics B-Proceedings Supplements 143, 492-492. 2005. Physics Letters B 591[1-6], 2004.

P092-05 "Effects of the interplay between interaction and disorder in bipartite entanglement"

Santos, L. F. and Rigolin, G.

We use a disordered antiferromagnetic spin-1/2 chain with anisotropic exchange coupling to model an array of interacting qubits. All qubits have the same level spacing, except two, which are called the defects of the chain. The level spacings of the defects are equal and much larger than all the others. We investigate how the entanglement between the two defects depends on the anisotropy of the system. When the anisotropy coupling is much larger than the energy difference between a defect and an ordinary qubit, the two defects become strongly entangled. Small anisotropies, on the contrary, may decrease the entanglement, which is, in this case, also much affected by the number of excitations. The analysis is made for nearest-neighbor and next-nearest-neighbor defects. The decrease in the entanglement for nearest neighbor defects is not very significant, especially in large chains

Physical Review A 71[3]. 032321. 2005.

P093-05 "Elastic and rotational excitation cross-sections for electron-water collisions in the low- and intermediate-energy ranges"

Machado, L. E., Brescansin, L. M., Iga, I., and Lee, M. T

We present a theoretical study on electron-H2O collisions in the low- and intermediate-energy ranges. More specifically, we report calculated elastic differential, integral and momentum transfer cross-sections as well as rotational excitation cross-sections in the (2-500)-eV range. In our calculations, an optical potential is used to represent the electron-molecule interaction. The Schwinger variational method combined with the distorted-wave approximation is used to solve the scattering equations. The comparison of our calculated results with other theoretical and/or experimental data available in the literature is very encouraging.

European Physical Journal D 33[2], 193-199. 2005.

P094-05 "Electron density and temperature determination using the concept of particle confinement time uniqueness"

Daltrini, A. M. and Machida, M.

The use of atomic hydrogen line emission to determine the particle confinement time τ(p) of a tokamak plasma is a well-known diagnostic technique. Using such a method, for any one of the emission lines, be it from Lyman, Balmer, or Paschen series, the same (i.e., unique) value of τ(p) must be obtained. Furthermore, this measurement is directly related to the local values of the electron temperature and density. We have developed a method based on the H-α, H-β, and H-γ hydrogen line emissions and on the concept of τ(p) uniqueness for a tokamak plasma, to determine the local electron density and temperature. The technique has been applied to plasma discharges generated in the NOVA-UNICAMP tokamak. The results show good agreement with measurements from multichannel Thomson scattering and Langmuir probe. A procedure to simulate the H-α emissivity radial profile using the obtained results is also discussed.

Review of Scientific Instruments 76[5]. 053508. 2005.

P095-05 "Evidence of formation of Si-C bonds during growth of Si-doped III-V semiconductor compounds"

Bettini, J. and de Carvalho, M. M. G

In this work, we demonstrate that Si-C bonds are formed in III-V semiconductor compounds grown by chemical beam epitaxy. Our results suggest that the formation of Si-C bonds occurs in III-V epitaxial layers with acceptor Carbon residual concentration and high Si concentrations (>10(17) cm(-3)). The main consequence of Si-C bonds is the generation of defects along [111] direction. These defects produce carrier concentration saturation, reduction of electrical mobility, crystal quality degradation, and surface defects.

Applied Physics Letters 86[15]. 152113. 2005.

P096-05 "Experimental and theoretical analyses of PrAl2 and NdAl2 composite for use as an active magnetic regenerator"

Carvalho, A. M. G., Campoy, J. C. P., Coelho, A. A., Plaza, E. J. R., Gama, S., and von Ranke, P. J.

We report the theoretical and experimental investigations on the magnetocaloric effect in the PrAl2 and NdAl2 compounds and a composite of these compounds for use as an active magnetic regenerator. The theoretical calculations were performed considering the crystalline electrical field anisotropy and the magnetocaloric potentials were calculated in the three main crystallographic directions. The experimental data, obtained for the polycrystalline samples, are in good agreement with the theoretical results. Also, an optimum molar fraction of the PrAl2 and NdAl2 composite was determined theoretically and experimentally and discussed in the framework of the optimum regeneration Ericsson cycle.

Journal of Applied Physics 97[8]. 083905-083905-5. 2005.

P097-05 "Experimental study of MR suspensions of carbonyl iron powders with different particle sizes"

Bombard, A. J. F., Alcantara, M. R., Knobel, M., and Volpe, P. L. O.

Magnetorheological suspensions (MRS) based on mixtures of two commercial carbonyl iron powders (BASF grades CL and SU) as magnetic phase and hydrocarbon oil as liquid phase were prepared. CL and SU are both soft magnetic powders, but CL is a coarse powder, while. SU is a fine one. The total mass fraction of iron was 80% w/w each formulation. Hydrophilic fumed silica (5% w/w of Aerosil (R) 2110) was used to reduce the settling. The mixing ratios were: CL 0%, CL 20%, CL 40%, CL 60%, CL 80% and CL 100%. A MRS, the mixture CL 80%, showed considerable reduction of the plastic viscosity without field, in the range of 100 - 500 s(-1), when compared to the MRS with just one powder. The yield stress values under applied field H - 340 kA/m were: 18.1 kPa for the MRS CL 0%, 18.3 kPa for the MRS's CL 20% and CL 40%, 20.0 kPa for the MRS CL 60%, 22.3 kPa for the MRS CL 80% and 23.3 kPa for the MRS CL 100%, respectively. For comparison, a sample of commercial MRF-132LD (Lord Corp.) in the same conditions showed yield value of 21.2 +/- 0.6 kPa. On the other hand, another MRS, CL 60%, showed an increment of similar to 33% on the normal force, with relation to the MRS prepared with just CL or just SU powders, above 150 kA/m. Therefore, mixing carbonyl iron powders with different particle sizes can improve the performance of MRS, decreasing the 'off' plastic viscosity, and increasing the MR effect

International Journal of Modern Physics B 19[7-9], 1332-1338. 2005.

P098-05 "Field-tuned quantum critical point in CeCoIn5 near the superconducting upper critical field"

Ronning, F., Capan, C., Bianchi, A., Movshovich, R., Lacerda, A., Hundley, M. F., Thompson, J. D., Pagliuso, P. G., and Sarrao, J. L.

We report a systematic study of high-magnetic-field specific heat and resistivity in single crystals of CeCoIn5 for the field oriented in the basal plane (H parallel to ab)of this tetragonal heavy fermion superconductor. We observe a divergent electronic specific heat as well as an enhanced A coefficient of the T-2 law in resistivity at the lowest temperatures, as the field approaches the upper critical field of the superconducting transition. Together with the results for field along the tetragonal axis (H parallel to c), the emergent picture is that of a magnetic-field-tuned quantum critical point which exists in the vicinity of the superconducting H-c2(0) despite a variation of a factor of 2.4 in H-c2(0) for different field orientations. This suggests that an underlying physical reason exists for the superconducting H-c2(0) to coincide with the quantum critical field. Moreover, we show that the recovery of a Fermi-liquid ground state with increasing magnetic field is more gradual, meaning that the fluctuations responsible for the observed quantum critical phenomena are more robust with respect to magnetic field, when the magnetic field is applied in plane. Together with the close proximity of the quantum critical point and H-c2(0) in CeCoIn5 for both field orientations, the anisotropy in the recovery of the Fermi-liquid state might constitute an important piece of information in identifying the nature of the fluctuations that become critical.

Physical Review B 71[10]. 104528. 2005.

P099-05 "Flavor and chiral oscillations with Dirac wave packets"

Bernardini, A. E. and De Leo, S.

We report about recent results on Dirac wave packets in the treatment of neutrino flavor oscillation where the initial localization of a spinor state implies an interference between positive and negative energy components of mass-eigenstate wave packets. A satisfactory description of fermionic particles requires the use of the Dirac equation as evolution equation for the mass eigenstates. In this context, a new flavor conversion formula can be obtained when the effects of chiral oscillation are taken into account. Our study leads to the conclusion that the fermionic nature of the particles, where chiral oscillations and the interference between positive and negative frequency components of mass-eigenstate wave packets are implicitly assumed, modifies the standard oscillation probability. Nevertheless, for ultrarelativistic particles and sharply peaked momentum distributions, we can analytically demonstrate that these modifications introduce correction factors proportional to m(1,2)(2)/p(0)(2) which are practically undetectable by any experimental analysis.

Physical Review D 71[7]. 076008. 2005.

P100-05 "Flavor and chiral oscillations"

Bernardini, A. E. and De Leo, S.

We seek a quantum-theoretic expression for the probability that a "fermionic" particle which is initially in a well-defined flavor, linear combination of mass-eigenstates, will be found, at later times, in another flavor state. We approach this problem by using the Dirac equation as evolution equation for the mass-eigenstates. The Dirac formalism is useful and essential in keeping clear many of the conceptual aspects of quantum oscillation phenomena that naturally arise in a relativistic spin one-half particle theory. Our study leads to the conclusion that the fermionic nature of the particles and the interference between positive and negative frequency components of mass-eigenstate wave packets modify the standard oscillation probability, obtained by implicitly assuming a "scalar" nature of the mass-eigenstates. Nevertheless, under particular assumptions, i.e. ultra relativistic particles, strictly peaked momentum distributions and minimal slippage, these modifications introduce correction factors proportional to m(1)(2),(2) /p(0)(2) practically un-detectable by any experimental analysis.

Modern Physics Letters A 20[9], 681-689. 2005.

P101-05 "High efficiency transfer of quantum information and multiparticle entanglement generation in translation-invariant quantum chains"

Plenio, M. B. and Semiao, F. L.

We demonstrate that a translation-invariant chain of interacting quantum systems can be used for high efficiency transfer of quantum entanglement and the generation of multiparticle entanglement over large distances and between arbitrary sites without the requirement of precise spatial or temporal control. The scheme is largely insensitive to disorder and random coupling strengths in the chain. We discuss harmonic oscillator systems both in the case of arbitrary Gaussian states and in situations when at most one excitation is in the system. The latter case, which we prove to be equivalent to an xy-spin chain, may be used to generate genuine multiparticle entanglement.

Such a 'quantum data bus' may prove useful in future solid state architectures for quantum information processing.

New Journal of Physics 7[73]. 2005.

P102-05 "Kinetics of excitonic complexes on tunneling devices"

Vercik, A., Gobato, Y. G., Camps, I., Marques, G. E., Brasil, M. J. S. P., and Makler, S. S.

In this work we have investigated the effects of trion formation on the tunneling current from both experimental and theoretical viewpoints. We have measured the current-voltage characteristics and the quantum-well photoluminescence emission of GaAs-Ga(l-x)Al(x)s n-i-n double barrier diodes. We have observed a preresonance shoulder in the current-voltage curve under high laser intensities associated with the formation of trions in the quantum well, which increase the number of free states in the resonant and excitonic levels, thus enhancing the tunneling mechanism. These excitonic complexes were detected through the photoluminescence spectra under bias. We have observed that the preresonance shoulder occurs under the same conditions for which a trion peak in the luminescence spectrum is present. This trion-assisted mechanism is terminated when neutral and charged excitons are dissociated either by thermal excitation or by scattering with free carriers in the quantum well. A phenomenological rate equation model has allowed us to confirm our assumptions on the effect of trion formation on the charge transport.

Physical Review B 71[7]. 075310. 2005.

P103-05 "Large-scale quantum effects in biological systems"

Von Mesquita, M. V., Vasconcellos, A. R., Luzzi, R., and Mascarenhas, S.

Particular aspects of large-scale quantum effects in biological systems, such as biopolymers and also microtubules in the cytoskeleton of neurons which can have relevance in brain functioning, are discussed. The microscopic (quantum mechanical) and macroscopic (quantum statistical mechanical) aspects, and the emergence of complex behavior, are described. This phenomena consists of the large-scale coherent process of Frohlich-Bose-Einstein condensation in open and sufficiently far-from-equilibrium biopolymers. Associated with this phenomenon is the presence of Schrodinger-Davydov solitons, which propagate, undistorted and undamped, when embedded in the Frohlich-Bose-Einstein condensate, thus allowing for the transmission of signals at long distances, involving a question relevant to bioenergetics.

International Journal of Quantum Chemistry 102[6], 1116-1130. 2005.

P104-05 "Low-temperature Al-induced crystallization of amorphous Ge"

Zanatta, A. R. and Chambouleyron, I.

This work reports on the low-temperature crystallization of hydrogenated amorphous germanium (a-Ge:H) films induced by aluminum. A series of aluminum-doped a-Ge:H films ([Al/Ge]similar to 10(-6)-10(-2) range) were deposited onto crystalline silicon substrates at 220 degrees C by the cosputtering technique under the same nominal conditions, except for the Al/Ge concentration. Raman scattering and infrared transmission spectroscopy were used for the structural characterization. The analysis of experimental data indicates that as-deposited Al-doped a-Ge:H films having an Al relative concentration between 1 and 2 at. % crystallize spontaneously. Aluminum contents below this range induce a partial crystallization of the films, whereas [Al/Ge]>2 at. % does not induce any crystallization. The mechanisms involved in the crystallization of these Al-doped a-Ge:H films were also investigated after thermal annealing treatments up to a temperature of 500 degrees C. Since the films are hydrogenated, the influence of hydrogen in the crystallization process was considered in detail. The ensemble of the data leads us to associate the induced crystallization with the coordination of, and the local order around, aluminum atoms in the a-Ge:H network. A microscopic mechanism behind the low-temperature crystallization is proposed. The present research indicates that both fourfold coordinated aluminum atoms and hydrogen species are fundamental in the crystallization phenomenon: the former acting as crystallization seeds, and the latter determining the dynamics of the process.

Journal of Applied Physics 97[9]. 094914-094914-11. 2005.

P105-05 "Low resolution structural study of two human HSP40 chaperones in solution - DjA1 from subfamily A and DjB4 from subfamily B have different quaternary structures"

Borges, J. C., Fischer, H., Craievich, A. F., and Ramos, C. H. I.

Proteins that belong to the heat shock protein (Hsp) 40 family assist Hsp70 in many cellular functions and are important for maintaining cell viability. A knowledge of the structural and functional characteristics of the Hsp40 family is therefore essential for understanding the role of the Hsp70 chaperone system in cells. In this work, we used small angle x-ray scattering and analytical ultracentrifugation to study two representatives of human Hsp40, namely, DjA1 (Hdj2/dj2/HSDJ/Rdj1) from subfamily A and DjB4 (Hlj1/DnaJW) from subfamily B, and to determine their quaternary structure. We also constructed low resolution models for the structure of DjA1-(1-332), a C-terminal-deleted mutant of DjA1 in which dimer formation is prevented. Our results, together with the current structural information of the Hsp40 C-terminal and J-domains, were used to generate models of the internal structural organization of DjA1 and DjB4. The characteristics of these models indicated that DjA1 and DjB4 were both dimers, but with substantial differences in their quaternary structures: whereas DjA1 consisted of a compact dimer in which the N and C termini of the two monomers faced each other, DjB4 formed a dimer in which only the C termini of the two monomers were in contact. The two proteins also differed in their ability to bind unfolded luciferase. Overall, our results indicate that these representatives of subfamilies A and B of human Hsp40 have different quaternary structures and chaperone functions.

Journal of Biological Chemistry 280[14], 13671-13681. 2005.

P106-05 "P 106- 05 "Magnetic and superconducting properties of $RuSr_2Gd1._5Ce_{0.5}Cu_2O_{10-\delta}$ samples: Dependence on the oxygen content and aging effects"

Cardoso, C. A., Lanfredi, A. J. C., Chiquito, A. J., Araujo-Moreira, F. M., Awana, V. P. S., Kishan, H., de Almeida, R. L., and de Lima, O. F.

The magnetic and superconducting properties of RuSr2Gd1.5Ce0.5Cu2O10-delta polycrystalline samples with different oxygen-doping levels are presented. A strong suppression of the superconducting temperature (T-c), as well as a reduction in the superconducting fraction, occurs as the oxygen content is reduced by annealing the samples in oxygen-deprived atmospheres. Drastic changes in the electrical resistivity are observed above T-c, possibly associated with oxygen removal, mainly from grain boundaries. However, the magnetic ordering is relatively less affected by the changes in oxygen content of the samples. The spin-glass transition is enhanced and shifted to higher temperatures with the reduction in oxygen content. This could be correlated with an increase in the spin disorder and frustration for the oxygen-depleted samples. Also, the same oxygen-vacancy-induced disorder could explain the reduction in the fraction of the sample showing antiferromagnetic order. We also report significant changes in the measured properties of the samples as a function of time.

Physical Review B 71[13]. 134509. 2005.

P107-05 "Magnetic properties of MnN: Influence of strain and crystal structure"

Marques, M., Teles, L. K., Scolfaro, L. M. R., Furthmuller, J., Bechstedt, F., and Ferreira, L. G.

For manganese mononitride (MnN), the total energy versus lattice constant is obtained using the spin density functional theory. Instead of the tetragonally distorted NaCl structure, we study the zinc blende and wurtzite structures in which AlN, GaN, and InN crystallize. The ground state with nonmagnetic, antiferromagnetic (AFM), or ferromagnetic (FM) arrangement of spins depends on the polymorph of MnN and on the lattice constant. At equilibrium lattice constants, in zinc blende it is AFM in [100] direction, and in wurtzite it is FM. The zinc blende polytype of MnN under hydrostatic pressure at the InN lattice constant presents FM ground state. For the wurtzite polytype at the GaN and AIN lattice constants, the AFM is the ground state, but goes back to a FM ground state for the InN lattice constants. For both, structures, the system presents a half-metallic state at InN lattice constants (with a total magnetic moment of 4 μ(B) per Mn atom) instead of the metallic state obtained for smaller lattice constants. Results indicate that the FM or the AFM state of Ga1-xMnxN and In1-xMnxN may be related to, relaxed, or strained, MnN incorporations or Mn-rich composition fluctuations.

Applied Physics Letters 86[16]. 164105. 2005.

P108-05 "Magnetically controlled impurities in quantum wires with strong Rashba coupling"

Pereira, R. G. and Miranda, E.

We investigate the effect of strong spin-orbit interaction on the electronic transport through nonmagnetic impurities in one-dimensional systems. When a perpendicular magnetic field is applied, the electron spin polarization becomes momentum-dependent and spin-flip scattering appears, to first order in the applied field, in addition to the usual potential scattering. We analyze a situation in which, by tuning the Fermi level and the Rashba coupling, the magnetic field can suppress the potential scattering. This mechanism should give rise to a significant magnetoresistance in the limit of large barriers.

Physical Review B 71[8]. 085318. 2005.

P109-05 "Multilevel ferromagnetic behavior of room-temperature bulk magnetic graphite"

Mombru, A. W., Pardo, H., Faccio, R., de Lima, O. F., Leite, E. R., Zanelatto, G., Lanfredi, A. J. C., Cardoso, C. A., and Araujo-Moreira, F. M.

In this paper we report on the magnetic properties of pure bulk ferromagnetic graphite, obtained by a chemical route previously described. This magnetic graphite has been obtained by a vapor reaction consisting of a controlled etching on the graphite structure. By magnetic force microscopy we have verified that its magnetic properties are related to the topographic defects introduced in the pristine material. Also, the magnetic properties have been verified through magnetization measurements as a function of temperature and applied magnetic field. At low temperatures (2 K) the saturation magnetization reaches a value of 0.58 emu/g, leading to a defect concentration of 1250 ppm. The system is highly irreversible due to the inhomogeneity of the distribution of defects in the material. Two transition temperatures are detected, T-c1=115(5) K and T-c2=315(5) K. These transitions could be associated to the weak coupling between ferromagnetic regions related to defects and to the ferromagnetism inside the defect regions.

Physical Review B 71[10]. 100404(R). 2005.

P110-05 "New analytical approximations for the Mathieu functions"

Dartora, C. A., Nobrega, K. Z., and Hernandez-Figueroa, H. E.

A new class of analytical tools to approximate even and odd Mathieu functions is examined. Our purpose is to contribute to decrease the lack of formulae for such approximations. In fact, the solutions here developed make possible approximations (using only few terms in a simple expansion) that are free of singularities and with no restriction in the x-domain.

Applied Mathematics and Computation 165[2], 447-458. 2005.

P111-05 "A new form of path integral for the coherent states representation and its semiclassical limit"

dos Santos, L. C. and de Aguiar, M. A. M.

The overcompleteness of the coherent states basis leads to a multiplicity of representations of Feynman's path integral. These different representations, although equivalent quantum mechanically, lead to different semiclassical limits. Two such semiclassical formulas were derived in [1] for the two corresponding path integral forms suggested by Klauder and Skagerstan in [2]. Each of these formulas involve trajectories governed by a different classical representation of the Hamiltonian operator: the P representation in one case and the Q representation in other. In this paper we construct a third representation of the path integral whose semiclassical limit involves directly the Weyl representation of the Hamiltonian operator, i.e., the classical Hamiltonian itself.

Brazilian Journal of Physics 35[1], 175-183. 2005.

P112-05 "New models of general relativistic static thick disks"

Vogt, D. and Letelier, P. S.

New families of exact general relativistic thick disks are constructed using the "displace, cut, fill, and reflect" method. A class of functions used to fill the disks is derived imposing conditions on the first and second derivatives to generate physically acceptable disks. The analysis of the function's curvature further restricts the ranges of the free parameters that allow physically acceptable disks. Then this class of functions together with the Schwarzschild metric is employed to construct thick disks in isotropic, Weyl and Schwarzschild canonical coordinates. In these last coordinates an additional function must be added to one of the metric coefficients to generate exact disks. Disks in isotropic and Weyl coordinates satisfy all energy conditions, but those in Schwarzschild canonical coordinates do not satisfy the dominant energy condition.

Physical Review D 71[8]. 084030. 2005.

P113-05 "Observation of the Xi(0) -> Sigma(+) mu(-)(nu)over-bar(mu) decay"

Gomes, R. A.

The KTeV experiment at Fermilab provides a good opportunity to investigate the neutral cascade semi-leptonic decays. The Xi(o) muon semi-leptonic decay, Xi(o) --> Sigma(-) mu(-)(nu) over bar (mu) is suppressed by phase space with only 21 MeV of release energy, making it difficult to be investigated. The study of this decay has a theoretical motivation since it provides another instance to test the Standard Model of particle physics. In this analysis we have observed the Xi(o) --> Sigma(+) mu(-) (nu) over bar (mu) decay and measured its Branching Ratio using Xi(o) --> Lambda pi(o) decay as the normalization mode.

Nuclear Physics B-Proceedings Supplements 142, 16-20. 2005.

P114-05 "Optical gain in a-SiNx : H < Nd >"

Tessler, L. R. and Biggemann, D.

We report optical gain measurements in neodymium-doped amorphous hydrogenated silicon sub-nitride (a-SiNx:H < Nd >) planar waveguides. Samples (1.5 mu m thick) were prepared by reactive rf-sputtering from a silicon target partially covered by metallic neodymium platelets using an Ar + N-2 + H-2 atmosphere. The substrates are oxidized (100) silicon wafers that are cleaved to define highly parallel flat waveguide faces. At low temperatures, the photoluminescence spectrum measured at the waveguide edge shows an increased and narrowed peak at 1130nm when compared with the spectrum taken in the direction of the guide top surface. The guided signal presents supralinear intensity dependence. An optical gain of 270 +/- 10cm(-1) was determined using the variable slit method exciting with a CW multiline Ar+ laser at 8kW/cm(2). The photon energy of the Ar+ laser lines is not resonant with any of the Nd3+ transitions, indicating that the excitation is efficiently transferred from the host to the rare earth ions. This result indicates that a-SiNx:H < Nd > can be used as an active optical medium.

Optical Materials 27[5], 769-772. 2005.

P115-05 "Organic modification of layered silicates: structural and thermal characterizations"

Prado, L. A. S. D., Karthikeyan, C. S., Schulte, K., Nunes, S. P., and de Torriani, I. L.

Organic modification of natural and synthetic layered silicates namely montmorillonite and laponite is reported in this work. The modified silicates are being subsequently used in the preparation of nano-composite membranes based on ionomers for fuel cells application. Laponite, an entirely synthetic silicate, was modified using organosiloxanes containing imidazole groups. Two different strategies were adopted for modification: (a) swelling of the silicate in 2-butanone followed by functionalization using the siloxane at room temperature, (b) direct reaction between laponite and the organosiloxane in xylene at 120 degrees C. Montmorillonite, a natural silicate, was supplied in the alkyl-ammonium form containing -OH groups. The modification of this silicate was conducted following the procedure (b). The structures of both plain and modified silicates were investigated by XRD showing that the interlayer distance (around 17 A) was not affected during the functionalization of laponite. However, a noticeable increase in the interlayer distance from 18.0 angstrom to 24.5 angstrom was observed for the modified montmorillonite. This clearly shows the presence of polysiloxane chains in between the silicate layers. Further characterization showed that the modification of these silicates was in the range between 16% and 23% (molar percentage). TGA was done between 25 and 300 degrees C in order to study the thermal degradation pattern of the silicates. The amount of adsorbed water could be determined from the results. The functionalization reduced the adsorption of water from 13.5% to 6.8% for laponite and from 8.5% to 40/o for montmorillonite.

Journal of Non-Crystalline Solids 351[12-13], 970-975. 2005.

P116-05 "Photoelectron diffraction studies of Cu on Pd(111) random surface alloys"

de Siervo, A., Soares, E. A., Landers, R., and Kleiman, G. G.

The study of surface alloys is motivated by their use in many applications of different segments of industry, such as in the search for new catalysts and sensors, in surface protection against corrosion, in lowering friction, and in testing electronic devices. An important aspect of surface alloys studies is that of the precise quantification of segregation and diffusion processes as well as the determination of surface structure. In this paper we report a combined low-energy electron diffraction and photoelectron diffraction (PED) (using synchrotron radiation) study of surface alloy formation when Cu ultrathin films are evaporated onto Pd(111) single-crystal surfaces. We present results for two different coverages (1 and 3 ML) and three annealing temperatures (300, 600, and 800 K). For these preparation conditions, a random alloy phase with different concentrations seems to form in the first few layers. Through the analysis of PED data performed using a multiple scattering formalism and the average T-matrix approximation it was possible to determine the atomic structure and the atomic concentration of the first three layers.

Physical Review B 71[11]. 115417. 2005.

P117-05 "Q penalties due to pump phase modulation and pump RIN in fiber optic parametric amplifiers with non-uniform dispersion"

Boggio, J. M. C., Guimaraes, A., Callegari, F. A., Marconi, J. D., and Fragnito, H. L.

We present an experimental and numerical investigation of the quality factor degradation (&UDelta; Q) due to pump phase modulation and pump relative intensity noise (RIN) in single- and double-pumped fiber optical parametric amplifiers (FOPAs). These penalties are investigated in FOPAs constructed with fibers having constant and randomly varying zero dispersion wavelength (λ(0)) along the fiber. We show that pump phase modulation in uniform fibers (constant λ(0)) produces large Q penalties, while in fibers with variations of λ(0), these penalties can be strongly reduced in both, single and double-pumped FOPAs. We also show that Q penalties due to pump phase modulation tend to disappear in FOPAs made with very short fibers (L < 0. 1 km) and very low dispersion slope (S-0 < 0.002 ps/nM(2) -km). The Q penalties due to pump RIN, which for typical FOPA parameters are much smaller than those due to pump phase modulation, are also reduced in non-uniform fibers (varying λ(0)), but do not depend on fiber length neither on fiber dispersion slope.

Optics Communications 249[4-6], 451-472. 2005.

P118-05 "Quantum teleportation of an arbitrary two-qubit state and its relation to multipartite entanglement"

Rigolin, G.

We explicitly show a protocol in which an arbitrary two qubit state vertical bar phi >=a vertical bar 00 >+b vertical bar 01 >+c vertical bar 10 >+d vertical bar 11 > is faithfully and deterministically teleported from Alice to Bob. We construct the 16 orthogonal generalized Bell states that can be used to teleport the two qubits. The local operations Bob must perform on his qubits in order to recover the teleported state are also constructed. They are restricted only to single-qubit gates. This means that a controlled-NOT gate is not necessary to complete the protocol. A generalization where N qubits are teleported is also shown. We define a generalized magic basis, which possesses interesting properties. These properties help us to suggest a generalized concurrence from which we construct a measure of entanglement that has a clear physical interpretation: A multipartite state has maximum entanglement if it is a genuine quantum teleportation channel.

Physical Review A 71[3]. 032303. 2005.

P119-05 "Quasi-bound states and intra-band transition energies in GaAs-(Ga,Al)As variably spaced semiconductor superlattices"

Reyes-Gomez, E., Oliveira, L. E., and Dios-Leyva, M.

A theoretical study of multi-quantum-well semiconductor heterostructures under applied electric fields perpendicular to the layers is performed within the transfer-matrix approach. Calculations are carried out for two different variably spaced superlattices.. designed in such a way that the conduction-electron states resonate at a certain value of the electric field. We have calculated the density of states for various values of the applied electric field, and results indicate a richly peaked structure associated to quasi-bound states of electrons, heavy holes and light holes. Results shown for the electric-field dependence of the interband transitions associated to electron-hole recombination indicate the possibility of a coherent resonant tunnelling, at a critical field, which may have applications in the design of more efficient solar-cell devices.

Physica B-Condensed Matter 358[1-4], 269-278. 2005.

P120-05 "Random initial condition in small Barabasi-Albert networks and deviations from the scale-free behavior"

Guimaraes, P. R., de Aguiar, M. A. M., Bascompte, J., Jordano, P., and dos Reis, S. F.

Barabasi-Albert networks are constructed by adding nodes via preferential attachment to an initial core of nodes. We study the topology of small scale-free networks as a function of the size and average connectivity of their initial random core. We show that these two parameters may strongly affect the tail of the degree distribution, by consistently leading to broad-scale or single-scale networks. In particular, we argue that the size of the initial network core and its density of connections may be the main responsible for the exponential truncation of the power-law behavior observed in some small scale-free networks.

Physical Review E 71[3]. 037101. 2005

P121-05 "Semiclassical limit of the entanglement in closed pure systems"

Angelo, R. M. and Furuya, K.

We discuss the semiclassical limit of the entanglement for the class of closed pure systems. By means of analytical and numerical calculations, we obtain two main results: (i) the short-time entanglement does not depend on Planck's constant and (ii) the long-time entanglement increases as more semiclassical regimes are attained. On one hand, this result is in contrast with the idea that the entanglement should be destroyed when the macroscopic limit is reached. On the other hand, it emphasizes the role played by decoherence in the process of emergence of the classical world. We also found that, for Gaussian initial states, the entanglement dynamics may be described by an entirely classical entropy in the semiclassical limit.

Physical Review A 71[4]. 042321. 2005.

P122-05 "Simultaneous recording of task-induced changes in blood oxygenation, volume, and flow using diffuse optical imaging and arterial spin-labeling MRI"

Hoge, R. D., Franceschini, M. A., Covolan, R. J. M., Huppert, T., Mandeville, J. B., and Boas, D. A.

Increased neural activity in brain tissue is accompanied by an array of supporting physiological processes, including increases in blood flow and the rates at which glucose and oxygen are consumed. These responses lead to secondary effects such as alterations in blood oxygenation and blood volume, and are ultimately the primary determinants of the amplitude and temporal signature of the blood oxygenation level-dependent (BOLD) signal used prevalently to map brain function. We have performed experiments using a combination of optical and MRI-based imaging methods to develop a more comprehensive picture of the physiological events accompanying activation of primary motor cortex during a finger apposition task. Temporal profiles for changes in tissue hemoglobin concentrations were qualitatively similar to those observed for MRI-based flow and oxygenation signals. Quantitative analysis of these signals revealed peak changes of +16 +/- 2% for HbO, - 13 2% for HbR, +8 +/- 3% for total Hb, +83 +/- 9% for cerebral blood flow, and +1.4 +/- 0.1% for the BOLD MRI signal. A mass balance model was used to estimate the change in rate of oxidative metabolism implied by the optical and flow measurements, leading to a computed value of +47 +/- 5%. It should be noted that the optical and MRI observations may in general reflect changes over different volumes of tissue. The ratio of fractional changes in oxidative metabolism to fractional change in blood flow was found to be 0.56 +/- 0.08, in general agreement with previous studies of flow-metabolism coupling.

Neuroimage 25[3], 701-707. 2005.

P123-05 "SiO2/PbTe quantum-dot multilayer production and characterization"

Rodriguez, E., Jimenez, E., Padilha, L. A., Neves, A. A. R., Jacob, G. J., Cesar, C. L., and Barbosa, L. C.

We report the fabrication of multilayer structures containing layers of PbTe quantum dots (QDs) spaced by 15-20 nm thick SiO2 layers. The QDs were grown by the laser ablation of a PbTe target using the second harmonic of Nd:YAG laser in an argon atmosphere. The SiO2 layers were fabricated by plasma chemical vapor deposition using tetramethoxysilane as a precursor. The influence of the ablation time on the size and size distribution of the QDs is studied by high-resolution transmission electron microscopy. Optical absorption measurements show clearly the QDs confinement effects.

Applied Physics Letters 86[11]. 113117. 2005.

P124-05 "Spontaneous decay rates in active waveguides"

Rieznik, A. A. and Rigolin, G.

We present a new method of measuring the guided, radiated, and total decay rates in uniform waveguides. It is also shown theoretically that large modifications of the total decay rate can be achieved in realistic erbium-doped fiber amplifiers and erbium-doped waveguide amplifiers with effective mode area radii smaller than &AP; 1 μ m.

Optics Letters 30[10], 1108-1110. 2005.

P125-05 "Structural and magnetic study of $LaBaCoCuO_{5+\delta}$"

Suescun, L., Jones, C. Y., Cardoso, C. A., Lynn, J. W., Toby, B. H., Araujo-Moreira, F. M., de Lima, O. F., Pardo, H., and Mombru, A. W.

The structure and magnetic properties of the compound LaBaCuCoO5+delta have been studied for the non-stoichiometric oxygen concentration delta approximate to 0.6. The structure is pseudo-cubic with a tripled perovskite unit cell. The crystal structure was determined by a combined Rietveld fit to neutron and synchrotron x-ray powder diffraction data in the

orthorhombic Pmmm space group, with cell parameters a=3.9223(3) angstrom, b=3.9360(3) angstrom, c=11.7073(8) angstrom, and V=180.74(2) angstrom(3) (room temperature). Antiferromagnetic ordering of Cu and Co magnetic moments is observed below 205(4) K. The magnetic structure with cell a(M)=2a, b(M)=2b, and c(M)=2c, could be described with the Shubnikov space group Fmmm'. The magnetic moments of both equivalent Cu/Co sites were determined at 50 and 170 K to be 0.83(3)mu(B) and 0.58(3)mu(B), respectively, consistent with one unpaired electron per atom. The fit of the intensities to a simple mean field magnetic model appeared to be insufficient to account for the variation of moments at temperatures close to T-N while a three dimensional Heisenberg model could improve the fit. Susceptibility measurements between 4 and 350 K also show irreversibility below 150 K. The local environments of Cu and Co were studied by extended x-ray absorption fine structure spectroscopy at both absorption edges. Cu atoms adopt an elongated octahedral or square-based pyramidal oxygen environment which suggests mainly the presence of Cu(II) in the structure. Co adopts different local environments, depending on the electronic and spin states

Physical Review B 71[14]. 144405.1-144405.9. 2005.

P126-05 "Superposition of monochromatic Bessel beams in (k(p), k(z))-plane to obtain wave focusing: Spatial localized waves"

Dartora, C. A., Nobrega, K. Z., Dartora, A., and Hernandez-Figueroa, H. E.

In this work we analyze the effect of superimposing monochromatic Bessel beams with different wave-vectors through the use of a multi-annular slit (or holographic methods). An analytical procedure based on the scalar diffraction theory allows one to obtain spatially localized waves.

Optics Communications 249[4-6], 407-413. 2005.

P127-05 "Theoretical investigation of optical properties in oligo(trans-1,2-di (2-thienyl) ethylene)"

Marcal, N. and Laks, B.

The electronic structures of poly(trans-1,2-di(2-thienyl)ethylene) (PTE) oligomers were theoretically analyzed following models based on neutral and charged oligomers for 1 < n < 7. Geometrical optimizations were carried out at the semiempirical level using parametric method 3 (PM3). For singly oxidized oligomer, the positive charge is concentrated around two central monomers. For doubly oxidized oligomer, the positive charge is concentrated around four central monomers. The energy of the electronic transitions and their associated oscillator strength values were also calculated for neutral and charged oligomers, so the UV-vis absorption spectra is presented. The calculations were done using the intermediate neglect of differential overlap Hamiltonian in combination with the single configuration-interaction technique in order to include correlations effects.

International Journal of Quantum Chemistry 103[5], 617-624. 2005.

P128-05 "Topics on high-energy elastic hadron scattering"

Menon, M. J.

We review the main results we have obtained in the area of high-energy elastic hadron scattering and presented in this series of Workshops on Hadron Interactions. After an introduction to some basic experimental and theoretical concepts, we survey the results reached by means of four approaches: analytic models, model-independent analyses, eikonal models and nonperturbative QCD. Some of the ongoing researches and future perspectives are also outlined

Brazilian Journal of Physics 35[1], 100-121. 2005.

P129-05 "Ultrafast optical switching with CdTe nanocrystals in a glass matrix"

Padilha, L. A., Neves, A. A. R., Rodriguez, E., Cesar, C. L., Barbosa, L. C., and Cruz, C. H. B.

This letter describes a principle demonstration of an ultrafast optical switch operating at 1 Tbit/s using CdTe-quantum-dots-doped glasses. Using a three-beam pump and probe experiment, we showed that thermal effects are responsible for a baseline in the pump and probe graphs and the nonexistence of carrier accumulation effects. After eliminating the thermal effects, we showed that, when two pump pulses are delayed by 1 ps, each pump pulse modulates the probe pulse independently, making this material highly promising for ultrafast all optical switching.

Applied Physics Letters 86[16]. 161111. 2005.

P130-05 "Uncertainty relation for the optimization of optical-fiber transmission systems simulations"

Rieznik, A. A., Tolisano, T., Callegari, F. A., Grosz, D. F., and Fragnito, H. L.

The mathematical inequality which in quantum mechanics gives rise to the uncertainty principle between two non commuting operators is used to develop a spatial step-size selection algorithm for the Split-Step Fourier Method (SSFM) for solving Generalized Non-Linear Schrodinger Equations (G-NLSEs). Numerical experiments are performed to analyze the efficiency of the method in modeling optical-fiber communications systems, showing its advantages relative to other algorithms.

Optics Express 13[10], 3822-3834. 2005.

P131-05 "Electricity generation: regulatory mechanisms to incentive renewable alternative energy sources in Brazil"

Carla Kazue Nakao Cavaliero*,Ennio Peres Da Silva

The dissemination of renewable alternative energy sources for electricity generation has always being done through regulatorymechanisms,created and managed by the government of each country.Since these sources are more costly to generate,they have received incentives in response to worldwide environmental concerns,above all with regard to the reduction of CO2 emissions. In Brazil,the electricity generation from renewable alternative sources is experiencing a new phase of growth.Until a short time ago,environmental appeal was the strongest incentive to these sources in Brazil but it was insuf .cient to attain its objective.With the electricity crisis and the rationing imposed in 2001,another important factor gained awareness:the need to diversify energy sources. Within this context,this work has the objective of analyzing the regulatory mechanisms recently developed to stimulate electricity generation from renewable alternative energy sources in Brazil by following the experience of other countries such as the United States,United Kingdom and Germany .

Energy Policy 33(13),1745-1752.2005

TRABALHOS ACEITOS PARA PUBLICAÇÃO

A001-05 "Statistical approach to fractal-structured systems: an illustratrion from the physics of semiconductor heterostructures."

A. R. Vasconcellos, E. Laureto, E. A. Meneses, and. R. Luzzi

Physico-chemical systems presenting fractal-life structures pose difficulties for their study eithin the scope of the standard statistical mechanics. A way around in order to make predictions for analyzing the system properties consists into resorting to auxiliary alternative statistics. We illustrate here one such a case in a study of luminescence spectra in nanometric quantum wells of semiconductor heterostructures which show anomalous behavior when compared with the usual one in bulk matter. This is a result of the occurrence of the phenomenon in contrained geometries(nanometer scales) with microroughened fractal-like boundaries. This sets practical difficulties for the theoretical treatment in that one does not have acess to a poper description of certain relevant characteristics of the system. The situation becomes further hard to deal with when the system is in far-from-equilibrium conditions.A way around to perform a study of the phenomenon consists into the use of a formalism for dealing with nonequilibrium many-body systems based on auxiliary statistics, and we resort here to Renyi approach adapted to a nonequilibrium statistical ensemble formalism.

Chaos, Solitons and Fractals 28[1], 8-19, 2006.

C001-05 "Planar waveguides prepared with organic-inorganic sol-gel derived from carboxylic acid solvolysis."

C Molina, S. J. L. Ribeiro, Y. Messaddeq, J. Flejlich.

Sol-gel processing offers a low temperature route for the development of organic-inorganic hybrid optical materials potentially suitable for the production of passive and active optical waveguides at low cost. Among many different precursors methacryloxypropyltrimethoxysilane (MAPTMS) hybrid is being used most due to the possibility of patterning using ultraviolet light radiation and lithographic techniques. Aiming waveguiding applications intrinsic optical losses at the NIR region are attributed overtones of the fundamental C-H stretching vibration. As a consequence most organic polymeric materials display important losses in that spectral region. Red shifting of the basic C-X strech (X=F, Cl, Br) by halogenation is one of the most useful approaches to overcome that problem. Another well known loss in optical waveguides comes from the residual O-H groups present in standard hybrid sol gel process using water to promote the hydrolysis. In this work we have prepared planar waveguides based on MAPTMS containing stable sol of zirconium oxide nanoparticles as a function as the 2,2,3,3-Tetrafluoropropylmethacrylate (TFPM) content. This monomer which contains photopolymerizable organic group and also C-F groups is used to increase the C-F concentration in the final material. Non-hydrolytic sol gel process by solvolysis route using acetic acid to decrease the O-H content was also used in this preparation. Moreover by using a non-hydrolytic process derived from carboxylic acid solvolysis we were able to avoid the O-H groups presence.

VII Brazilian Symposiun on Glass and related Materials - 2005

Abstracta

Instituto de Física
Diretor: Prof. Dr. Júlio Cesar Hadler Neto
Universidade Estadual de Campinas - UNICAMP
Cidade Universitária C.P. 6165
CEP: 13081-970 - Campinas - SP - Brasil
e-mail: secdir@ifi.unicamp.br
Fone: 0XX 19 3521-5300

Publicação

Biblioteca do Instituto de Física Gleb Wataghin
http://webbif.ifi.unicamp.br
Diretora Técnica: Rita Aparecida Sponchiado

Elaboração
Tânia Macedo Folegatti
absctact@ifi.unicamp.br

Projeto Gráfico
ÍgneaDesign

Impressão

Gráfica Central - Unicamp